

Purdue University Purdue e-Pubs

Department of Electrical and Computer
Engineering Faculty Publications

Department of Electrical and Computer
Engineering

2015

Bifacial Si heterojunction-perovskite organic-inorganic tandem to produce highly efficient ($\eta T^* \sim 33\%$) solar cell

Reza Asadpour

Purdue University, rasadpou@purdue.edu

Raghu Vamsi Krishna Chavali

Purdue University, raghu.vamsi.k.chavali.1@purdue.edu


Mohammad Ryyan Khan

Purdue University, ryyan.khan.eee@gmail.com

Muhammad Ashraful Alam

Purdue University, alam@purdue.edu

Follow this and additional works at: <https://docs.lib.purdue.edu/ecepubs>

 Part of the [Electronic Devices and Semiconductor Manufacturing Commons](#), and the [Other Electrical and Computer Engineering Commons](#)

Asadpour, Reza; Chavali, Raghu Vamsi Krishna; Khan, Mohammad Ryyan; and Alam, Muhammad Ashraful, "Bifacial Si heterojunction-perovskite organic-inorganic tandem to produce highly efficient ($\eta T^* \sim 33\%$) solar cell" (2015). *Department of Electrical and Computer Engineering Faculty Publications*. Paper 71.
<https://docs.lib.purdue.edu/ecepubs/71>

This document has been made available through Purdue e-Pubs, a service of the Purdue University Libraries. Please contact epubs@purdue.edu for additional information.

Bifacial Si heterojunction-perovskite organic-inorganic tandem to produce highly efficient ($\eta T^* \sim 33\%$) solar cell

Reza Asadpour, Raghu V. K. Chavali, M. Ryyan Khan, and Muhammad A. Alam

Citation: *Applied Physics Letters* **106**, 243902 (2015); doi: 10.1063/1.4922375

View online: <http://dx.doi.org/10.1063/1.4922375>

View Table of Contents: <http://scitation.aip.org/content/aip/journal/apl/106/24?ver=pdfcov>

Published by the **AIP Publishing**

Articles you may be interested in

The role of a LiF layer on the performance of poly(3,4-ethylenedioxythiophene):poly(styrenesulfonate)/Si organic-inorganic hybrid solar cells

Appl. Phys. Lett. **104**, 083514 (2014); 10.1063/1.4866968

Amorphous silicon oxide window layers for high-efficiency silicon heterojunction solar cells

J. Appl. Phys. **115**, 024502 (2014); 10.1063/1.4861404

Enhanced charge collection in confined bulk heterojunction organic solar cells

Appl. Phys. Lett. **99**, 163301 (2011); 10.1063/1.3651509

Towards a high efficiency amorphous silicon solar cell using molybdenum oxide as a window layer instead of conventional p-type amorphous silicon carbide

Appl. Phys. Lett. **99**, 063504 (2011); 10.1063/1.3624591

High efficiency double heterojunction polymer photovoltaic cells using highly ordered TiO₂ nanotube arrays

Appl. Phys. Lett. **91**, 152111 (2007); 10.1063/1.2799257

Frustrated by old technology? Is your AFM dead and can't be repaired? Sick of bad customer support?

It is time to upgrade your AFM
Minimum \$20,000 trade-in discount
for purchases before August 31st

**Asylum Research is today's
technology leader in AFM**

dropmyoldAFM@oxinst.com

OXFORD
INSTRUMENTS
The Business of Science®



Bifacial Si heterojunction-perovskite organic-inorganic tandem to produce highly efficient ($\eta_T^* \sim 33\%$) solar cell

Reza Asadpour,^{a)} Raghu V. K. Chavali,^{a)} M. Ryyan Khan,^{a)} and Muhammad A. Alam^{b)}
Electrical and Computer Engineering Department, Purdue University, West Lafayette, Indiana-47907, USA

(Received 7 January 2015; accepted 31 May 2015; published online 17 June 2015)

As single junction photovoltaic (PV) technologies, both Si heterojunction (HIT) and perovskite based solar cells promise high efficiencies at low cost. Intuitively, a traditional tandem cell design with these cells connected in series is expected to improve the efficiency further. Using a self-consistent numerical modeling of optical and transport characteristics, however, we find that a traditional series connected tandem design suffers from low J_{SC} due to band-gap mismatch and current matching constraints. Specifically, a traditional tandem cell with state-of-the-art HIT ($\eta = 24\%$) and perovskite ($\eta = 20\%$) sub-cells provides only a modest tandem efficiency of $\eta_T \sim 25\%$. Instead, we demonstrate that a bifacial HIT/perovskite tandem design decouples the optoelectronic constraints and provides an innovative path for extraordinary efficiencies. In the bifacial configuration, the same state-of-the-art sub-cells achieve a normalized output of $\eta_T^* = 33\%$, exceeding the bifacial HIT performance at practical albedo reflections. Unlike the traditional design, this bifacial design is relatively insensitive to perovskite thickness variations, which may translate to simpler manufacture and higher yield.

© 2015 AIP Publishing LLC. [<http://dx.doi.org/10.1063/1.4922375>]

In recent years, the search for low-cost highly efficient solar cells has resulted in two cell technologies (inorganic a-Si/c-Si Heterojunction (HIT) and organic perovskite) with comparable, but complementary characteristics. On the one hand, the standard a-Si/c-Si HIT technology is poised to capture a significant proportion of traditional c-Si solar cells due to its high efficiency and better temperature coefficients.^{1,2} On the other hand, the recent dramatic gain in efficiency of perovskite cells promises to finally realize the presumed cost advantages of organic solar cells.³⁻⁵ With significant efforts in device analysis⁶⁻¹¹ and optimization,¹²⁻¹⁵ several groups have achieved high efficiency ($\eta \geq 22\%$) HIT cells.¹⁶ Similarly, with improvement in processing and material quality, state-of-the-art perovskite cells have reached an efficiency of $\sim 20\%$.¹⁷⁻¹⁹

A perovskite/HIT tandem design that can suppress individual bottlenecks and take advantage of their complementary characteristics may improve the efficiency further. Recently, the efficiency gain of tandem designs with perovskite as the top cell and a range of bottom cells have been explored. Using a *four* terminal configuration, Bailie *et al.*²⁰ obtained 17% and 18.6% efficient tandem cells with mc-Si ($\eta \sim 11\%$) and copper indium gallium selenide (CIGS, $\eta \sim 17\%$) bottom cells, respectively. Similarly, Löper *et al.*²¹ obtained a 13.4% efficient tandem cell with (presumably) a highly efficient a-Si:H/c-Si heterojunction bottom cell using the same configuration. Finally, Mailoa *et al.*²² used a c-Si bottom cell in a two terminal tandem design to demonstrate a 13.7% cell. These studies indicate that a poor performing top cell can significantly limit the performance of traditional tandem cell designs. Indeed, the tandem efficiency may saturate for the state-of-art sub-cells.

There have been some efforts to predict the theoretical limits for these traditional tandem designs using perovskite sub-cell on top of c-Si²³ or a-Si/c-Si heterojunction bottom cell.²⁴ These studies are not self-consistent; rather, they rely only on optical modeling. The conclusions based on carrier transport modelled by a simple one-diode compact model may not be definitive, at least in the case of a-Si/c-Si heterojunction solar cells.⁸

From the above discussion, we observe that there have been some efforts to improve the practical conversion efficiency using the traditional tandem designs, however, the efficiency gains are not significant. Indeed, theoretical limits based on full self-consistent optoelectronic simulations are still lacking. In this letter, using detailed optical and carrier transport modeling, first, we re-explore the traditional tandem cell design. Starting from state-of-the-art cell parameters for the sub-cells ($\sim 20\%$ efficient perovskite cell, $\sim 24\%$ efficient HIT cell), an optimized tandem cell offers only a modest improvement, $\eta_T \sim 25\%$. Moreover, the optimization dictates a strict control over the perovskite layer thickness: even a ~ 20 nm deviation from the optimum thickness would degrade the net efficiency by 1%, negating the rationale for a tandem cell.

Instead, we suggest that another design involving a HIT and perovskite *bifacial* tandem cells can circumvent the constraints of the traditional design, and increase the *normalized* output to $\eta_T^* \sim 33\%$ (output power normalized to 1-sun illumination, that is, for 1000 W/m² input power, 330 W/m² output power is expected.). Indeed, the bifacial tandem would outperform the bifacial HIT cell for typical albedo reflection ($R_A < 40\%$). Further, the bifacial tandem design would be insensitive to the sub-cell thickness variation which obviates the need for layer optimization. The output gain is not restricted to state-of-the-art champion cells; even sub-optimal perovskite cell and standard HIT cell would benefit substantially from this strategy (see the supplementary material for details).²⁵

^{a)}The authors contributed equally to this work.

^{b)}Electronic mail: alam@purdue.edu

For this study, we consider a perovskite solar cell with the absorber layer ($\text{CH}_3\text{NH}_3\text{PbI}_3$) sandwiched between poly(3,4-ethylenedioxythiophene) polystyrene sulfonate (PEDOT:PSS) hole transport material (HTM) and phenyl-C₆₁-butyric acid methyl ester (PCBM) electron transport material (ETM).^{3,26} This perovskite sub-structure is then contacted by ITO and Al. The HIT cell uses c-Si as the active material, with p⁺ and n⁺ doped a-Si passivation layers acting as the emitter (i.e., HTM) and the back surface field (ETM), respectively. The cell is contacted with ITO at the front and ITO/Al at the back.

The traditional tandem cell consists of the higher bandgap perovskite ($E_G^{\text{PVK}} \approx 1.55 \text{ eV}$) sub-structure stacked on top of the lower bandgap ($E_G^{\text{cSi}} \approx 1.12 \text{ eV}$) c-Si HIT-sub-cell (see Fig. 1(b)). The bifacial tandem cell has a similar design except for the absence of an Al back contact. This allows the absorption of light reflected from the ground, as shown in Fig. 1(c). We will consider both traditional and bifacial tandem designs, to demonstrate why and how bifacial tandem design outperforms the traditional design.

The absorption spectrum and the spatial photo-generation profile in the layered solar cell structure is calculated by solving the Maxwell's equations using the Transfer Matrix Method (TMM).²⁷ Illumination of AM 1.5G solar

spectrum over the wavelength range of 300–1500 nm is used in this simulation. The materials in different layers of the cell are characterized by experimentally measured absorption coefficient and refractive indices reported in the literature.^{25,28–30} For this study, we assume planar structures. For the bifacial tandem, a perfect antireflective coating is assumed at the back (not shown in Fig. 1(c), see the supplementary material²⁵ for details).

The transport of the charged carriers (electrons and holes) is modeled by the generalized drift-diffusion formalism,³¹ using MEIDCI™ device simulator.³² The contacts are presumed ohmic. See Table S1 for model equations, and Tables S2 and S3 for simulation parameters in the supplementary material.²⁵ The parameters are consistent with literature yielding in experimentally observed device characteristics.

To model the tandem cell designs, first, we perform optical simulations of the *full* structure. Then, the carrier generation profiles so obtained are used in the transport simulator to separately characterize $J - V$ for the sub-cells. Finally, the sub-cells are connected in series using a circuit model (with negligible series resistance) to obtain the final $J - V$ characteristics of the tandem cell.

The electronic properties of the materials (perovskite, a-Si, and c-Si) considered in this study are chosen in such a way that we obtain the state-of-the-art efficiencies of 24% for HIT cell and 20% for the perovskite cell (see Tables S2 and S3 in the supplementary material for parameter list).²⁵ The corresponding $J - V$ characteristics are provided in Fig. 3(a). In the following discussions, we will show how these two technologies can be arranged in tandem to achieve high performance solar cells.

For a traditional tandem solar cell, a sufficiently thick top sub-cell should absorb *all the photons* above its bandgap, transmitting the rest of the solar spectrum to the bottom cell. The bottom sub-cell then absorbs above its bandgap from the remaining part of the spectrum. The optimum bandgap for the top cell is selected such that the sub-cell currents are matched and output power is maximized. Ideally, a top cell with $E_G \sim 1.7 \text{ eV}$ is required to match current produced by the c-Si bottom sub-cell, to achieve the maximum efficiency for the combination.³³

Unfortunately, in the case of the perovskite/HIT series tandem cell (see Fig. 1(b)), the perovskite bandgap (1.55 eV) is considerably smaller than the optimum bandgap of the top-cell ($E_G \sim 1.7 \text{ eV}$).³³ This makes the traditional tandem design sub-optimal because 300–400 nm thick typical perovskite top-cell would absorb so many photons that the bottom HIT cell (c-Si absorber) would not be able to produce sufficient J_{SC} . This mismatch in J_{SC} dramatically suppresses the power output from the tandem cell. Even for a relatively thin top-cell (e.g., $L_{\text{PVK}} \sim 170 \text{ nm}$, see Fig. 2), the currents are mismatched by 4 mA/cm^2 (red line, $J_{\text{abs}}^{\text{cSi}}$, green line, $J_{\text{abs}}^{\text{PVK}}$). Therefore, a delicate thickness control is *essential* in designing the traditional tandem cell with these mismatched sub-cells.

Fig. 2 shows that the sub-cell currents can be matched by varying the thickness of the perovskite (L_{PVK}) layer. The minimum absorption between the two sub-cells approximately defines the tandem cell J_{SC} . Therefore, we maximize

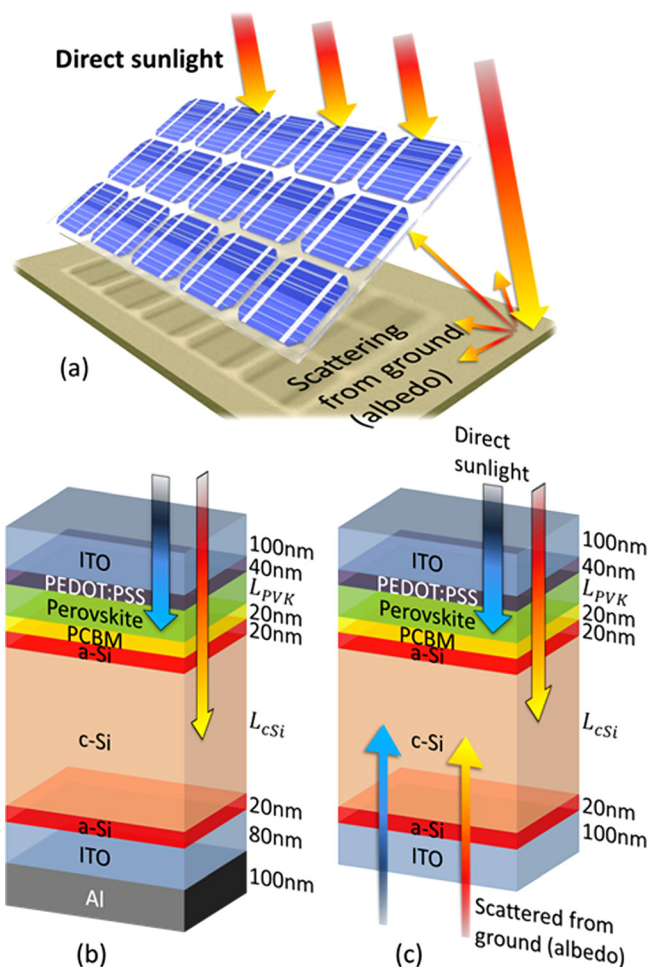


FIG. 1. (a) A solar panel generally utilizes the direct illumination of sunlight. A fraction of the light can also be scattered from the ground onto the back of the panel. (b) Traditional tandem structure and (c) a bifacial tandem structure.

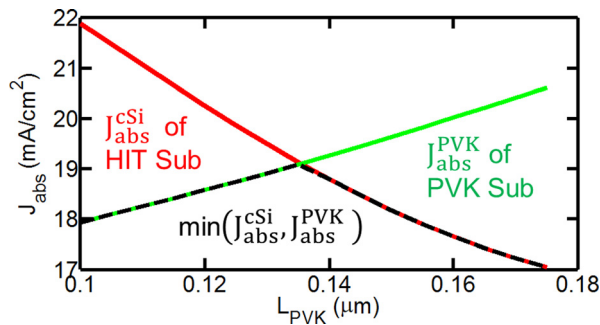


FIG. 2. Absorbed sunlight (in terms of corresponding current density J_{abs}) is shown for perovskite (green) and HIT (red) sub-cells as a function of L_{PVK} . The J_{SC} of the series tandem cell will be limited to $\min(J_{abs}^{cSi}, J_{abs}^{PVK})$, as shown by the dashed black lines. L_{cSi} is set to $200\mu\text{m}$.

$\min(J_{abs}^{PVK}, J_{abs}^{cSi})$ for achieving the highest overall current (black dashed line in Fig. 2). As the sensitivity of J_{SC} ($\sim \min(J_{abs}^{PVK}, J_{abs}^{cSi})$) on the c-Si layer thickness is negligible, $L_{cSi} = 200\mu\text{m}$ in HIT cell is chosen for the optimized tandem cell. In contrast, the matched current is highly sensitive to L_{PVK} and even 20 nm variation will lead to more than 1 mA/cm² lowering of short circuit current—this translates to more than 1% loss in tandem cell efficiency. The optical simulation indicates that the efficiency would be optimal at $L_{PVK} = 135\text{ nm}$ (see absorption spectrum in Fig. S2 in the supplementary material).²⁵

Once the cell thicknesses are determined from optical simulation, the analysis of carrier transport produces the full $J - V$ characteristics. First, consider the individual $J - V$ characteristics of perovskite and HIT cells, as shown in Fig. 3(a). The HIT solar cell has a higher J_{SC} but lower V_{OC} compared to the perovskite cell (as $E_G^{cSi} < E_G^{PVK}$). In a tandem structure, the sub-cell currents must be matched, as shown in Fig. 3(b). J_{SC} in the tandem cell ($\sim 18\text{ mA/cm}^2$) after current matching is lower than both the perovskite ($\sim 24.5\text{ mA/cm}^2$) and the HIT ($\sim 40.5\text{ mA/cm}^2$) cells. The V_{OC} of the tandem cell adds up to $\sim 1.65\text{ V}$ from the sub-cells. The total efficiency is $\eta_T \sim 25\%$, which is only slightly higher than the individual cells, $\eta_{HIT} \sim 24\%$ and $\eta_{PVK} \sim 20\%$. Therefore, with careful layer optimization, it is possible to obtain modest efficiency gains through traditional tandem configurations; however, it may not be cost effective.

In practice, it is difficult to control L_{PVK} within 20–30 nm by spin or drop-casting, causing the average gain to be much lower than the optimal. Also, in a tandem cell,

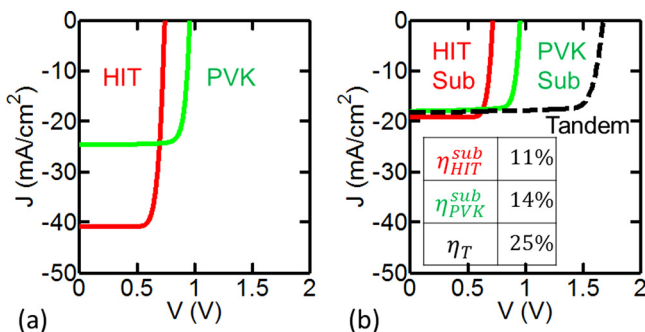


FIG. 3. $J - V$ characteristics of (a) individual HIT and perovskite cells (b) HIT (red) and perovskite (green) sub-cell $J - V$ characteristics are shown along with the tandem cell (black dashed line). Inset table shows sub-cell contribution to the efficiency.

the sub-cells underperform compared to their individual limits ($\eta_{PVK}^{sub} \sim 14\%$ vs. $\eta_{PVK} \sim 20\%$; $\eta_{HIT}^{sub} \sim 11\%$ vs. $\eta_{HIT} \sim 24\%$). A reduced coupling between the sub-cells is desired and the characteristic bifacial configuration of the HIT cell (see Fig. 1(c)) offers a simple solution, with normalized output $\eta_T^* \rightarrow 33\%$ (output power normalized to 1-sun illumination), as discussed below.

The bifacial design allows light to enter the device from both top and bottom faces. In a HIT cell, the back ITO must be inserted between a-Si and metal contact to improve the optical properties and reliability³⁴ so that a transparent back-contact is available at no extra cost. Fig. 1(a) shows that the bifacial panel accepts direct solar illumination from the front and albedo reflected light from the background (grass, concrete, snow, etc.). The traditional and the bifacial perovskite-HIT tandem are identical (Fig. 1(b) vs. 1(c)), except for the back Al contact. As a result, slight increase in series resistance is expected for the bifacial design; for this study, we assume that this effect is negligible.

The front side of the cell is exposed to direct sunlight—the high energy part of the spectrum with energies $> E_G^{PVK}$ (1.55 eV) is now mostly absorbed in a 350 nm perovskite sub-cell (see absorption spectrum in Fig. S3 in the supplementary material).²⁵ The bottom HIT sub-cell absorbs few photons from the remaining spectrum (see the blue line in Fig. 4). In a typical tandem, with no albedo reflectance ($R_A = 0$), η_T^* would be severely affected. However, the partially reflected light from the ground/surroundings, characterized by the albedo reflectance ($R_A < 100\%$), improves photo-generation in the HIT sub-cell considerably (red dashed line in Fig. 4). For the traditional tandem cell discussed earlier, η_T was limited by the constraint of matched sub-cell currents. Since the bifacial tandem cell improves J_{SC}^{HIT} , one can use a thicker perovskite to improve J_{SC}^{PVK} , free from typical constraints of a tandem cell, i.e., restriction on L_{PVK} vs. L_{cSi} . For this analysis, we choose these thicknesses to be 350 nm and $200\mu\text{m}$, respectively.

We can now compare the bifacial HIT cell and the bifacial tandem for varying R_A . For low R_A ($< 20\%$), the perovskite has higher current than the HIT sub-cell (see Fig. 5(a)), and the efficiency is limited by the HIT cell. As we increase scattered light entering through the bottom cell, the absorption in the HIT sub-cell will increase linearly with R_A . However, the tandem J_{SC} will be limited by the lower of the two sub-cells currents, shown by the black line in Fig. 5(a). Beyond $R_A > 20\%$, the tandem current is limited by the perovskite sub-cell. This also explains why the tandem cell

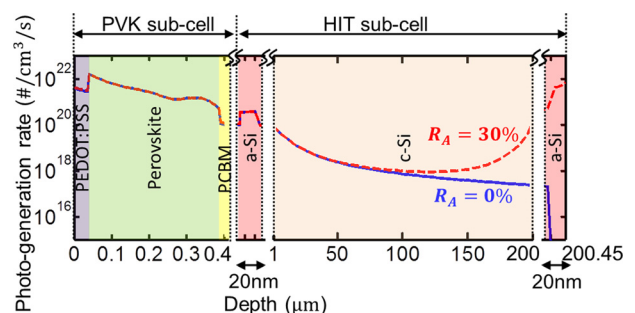


FIG. 4. Spatial photo-generation profile in the tandem cell. The primary sunlight is from the left.

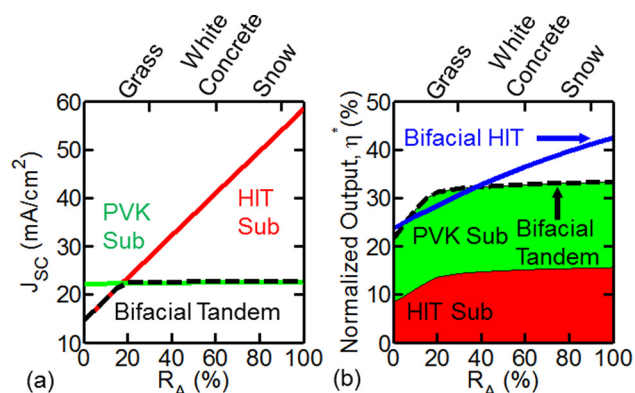


FIG. 5. (a) J_{sc} of the sub-cells and the bifacial tandem cell as function of albedo R_A is shown. (b) Output η^* (normalized to 1-sun) of the perovskite and the HIT sub-cells (green and red areas) are shown. The bifacial tandem (black dashed line) outperforms the bifacial HIT cell (blue solid line) for $R_A < 40\%$. Common backgrounds such as grass, white concrete, and snow have R_A of approximately 30%, 60%, and 90%, respectively.^{25,35}

output η_T^* increases with R_A and then saturates to $\sim 33\%$ beyond $R_A > 20\%$ (see Fig. 5(b)). Further, from Fig. 5(b) we observe that for a practical range of $R_A < 40\%$ the tandem design (black line) outperforms the typical bifacial HIT cell (blue solid line) by a considerable margin. Obviously, this bifacial design requires a slightly modified stacking of the cells—a suggested process flow is described in the supplementary material.²⁵

To summarize, in this paper we have explored the performance potential of perovskite-HIT tandem cell based on state-of-the-art sub-cells. We find that a traditional tandem design requires an optimized perovskite thickness of $L_{PVK} \sim 135$ nm to provide a modest 25% efficient cell. Unfortunately, the efficiency gain is compromised due to sensitivity to L_{PVK} and both the cells underperform compared to their individual efficiencies. A bifacial tandem design resolves the current matching problem and improves the performance to 33%. As an added advantage, this efficiency gain is insensitive to thicknesses of perovskite and c-Si layers. Further, it outperforms the bifacial HIT cell over a practical range of albedo reflection. Therefore, it offers a viable, robust HIT-perovskite tandem for low-cost, highly efficient PV technology.

We gratefully acknowledge research support from the Bay Area PV Consortium (a Department of Energy project with Prime Award number DE-EE0004946), and by the US-India Partnership to Advance Clean Energy-Research (PACE-R) for the Solar Energy Research Institute for India and the United States (SERIUS), a joint program by U.S. Department of Energy and the Government of India.

¹K. Maki, D. Fujishima, H. Inoue, Y. Tsunomura, T. Asaumi, S. Taira, T. Kinoshita, M. Taguchi, H. Sakata, H. Kanno, and E. Maruyama, in *Proceedings of the 37th IEEE Photovolt. Spec. Conf.* (IEEE, 2011), pp. 000057–000061.

²M. Taguchi, A. Yano, S. Tohoda, K. Matsuyama, Y. Nakamura, T. Nishiwaki, K. Fujita, and E. Maruyama, *IEEE J. Photovoltaics* **4**, 96 (2014).

- ³J. You, Z. Hong, Y. (Michael) Yang, Q. Chen, M. Cai, T.-B. Song, C.-C. Chen, S. Lu, Y. Liu, H. Zhou, and Y. Yang, *ACS Nano* **8**, 1674 (2014).
- ⁴P. Docampo, J. M. Ball, M. Darwich, G. E. Eperon, and H. J. Snaith, *Nat. Commun.* **4**, 2761 (2013).
- ⁵P. P. Boix, K. Nonomura, N. Mathews, and S. G. Mhaisalkar, *Mater. Today* **17**, 16 (2014).
- ⁶A. S. Gudovskikh and J. P. Kleider, *Appl. Phys. Lett.* **90**, 034104 (2007).
- ⁷R. S. Crandall, E. Iwaniczko, J. V. Li, and M. R. Page, *J. Appl. Phys.* **112**, 093713 (2012).
- ⁸R. V. K. Chavali, J. R. Wilcox, B. Ray, J. L. Gray, and M. A. Alam, *IEEE J. Photovoltaics* **4**, 763 (2014).
- ⁹R. Varache, J. P. Kleider, W. Favre, and L. Korte, *J. Appl. Phys.* **112**, 123717 (2012).
- ¹⁰S. De Wolf and M. Kondo, *Appl. Phys. Lett.* **90**, 042111 (2007).
- ¹¹R. V. K. Chavali, S. Khatavkar, C. V. Kannan, V. Kumar, P. R. Nair, J. L. Gray, and M. A. Alam, *IEEE J. Photovoltaics* **5**, 725 (2015).
- ¹²L. Korte, E. Conrad, H. Angermann, R. Stangl, and M. Schmidt, *Sol. Energy Mater. Sol. Cells* **93**, 905 (2009).
- ¹³H. Angermann, L. Korte, J. Rappich, E. Conrad, I. Sieber, M. Schmidt, K. Hübener, and J. Hauschild, *Thin Solid Films* **516**, 6775 (2008).
- ¹⁴A. Descocudres, L. Barraud, S. De Wolf, B. Strahm, D. Lachenal, C. Guérin, Z. C. Holman, F. Zicarelli, B. Demareux, J. Seif, J. Holovsky, and C. Ballif, *Appl. Phys. Lett.* **99**, 123506 (2011).
- ¹⁵Z. C. Holman, A. Descocudres, L. Barraud, F. Z. Fernandez, J. P. Seif, S. De Wolf, and C. Ballif, *IEEE J. Photovoltaics* **2**, 7 (2012).
- ¹⁶C. Ballif, S. De Wolf, A. Descocudres, and Z. C. Holman, *Advances in Photovoltaics: Part 3* (Elsevier, 2014), pp. 73–120.
- ¹⁷H. Zhou, Q. Chen, G. Li, S. Luo, T. Song, H.-S. Duan, Z. Hong, J. You, Y. Liu, and Y. Yang, *Science* **345**, 542 (2014).
- ¹⁸M. A. Green, K. Emery, Y. Hishikawa, W. Warta, and E. D. Dunlop, *Prog. Photovoltaics Res. Appl.* **23**, 1 (2015).
- ¹⁹W. Nie, H. Tsai, R. Asadpour, J.-C. Blancon, A. J. Neukirch, G. Gupta, J. J. Crochet, M. Chhowalla, S. Tretiak, M. A. Alam, H.-L. Wang, and A. D. Mohite, *Science* **347**, 522 (2015).
- ²⁰C. D. Bailie, M. G. Christoforo, J. P. Mailoa, A. R. Bowering, E. L. Unger, W. H. Nguyen, J. Burschka, N. Pellet, J. Z. Lee, M. Grätzel, R. Noufi, T. Buonassisi, A. Salleo, and M. D. McGehee, *Energy Environ. Sci.* **8**, 956 (2015).
- ²¹P. Löper, S.-J. Moon, S. Martín de Nicolas, B. Niesen, M. Ledinsky, S. Nicolay, J. Bailat, J.-H. Yum, S. De Wolf, and C. Ballif, *Phys. Chem. Chem. Phys.* **17**, 1619 (2014).
- ²²J. P. Mailoa, C. D. Bailie, E. C. Johlin, E. T. Hoke, A. J. Akey, W. H. Nguyen, M. D. McGehee, and T. Buonassisi, *Appl. Phys. Lett.* **106**, 121105 (2015).
- ²³B. W. Schneider, N. N. Lal, S. Baker-Finch, and T. P. White, *Opt. Express* **22**, A1422 (2014).
- ²⁴M. Filipič, P. Löper, B. Niesen, S. De Wolf, J. Krč, C. Ballif, and M. Topič, *Opt. Express* **23**, A263 (2015).
- ²⁵See supplementary material at <http://dx.doi.org/10.1063/1.4922375> for perovskite (n, k) Fig. S1, absorption spectrum Figs. S2–S4, moderate cell/sub-cell results Figs. S5–S8, energy band diagrams Figs. S9 and S10, transport equations, parameters Tables S1–S3 and Table S4 for albedo reflection of common materials.
- ²⁶J. Seo, S. Park, Y. Chan Kim, N. J. Jeon, J. H. Noh, S. C. Yoon, and S. I. Seok, *Energy Environ. Sci.* **7**, 2642 (2014).
- ²⁷L. A. A. Pettersson, L. S. Roman, and O. Inganäs, *J. Appl. Phys.* **86**, 487 (1999).
- ²⁸V. S. Gevaerts, L. J. A. Koster, M. M. Wienk, and R. A. J. Janssen, *ACS Appl. Mater. Interfaces* **3**, 3252 (2011).
- ²⁹H. Hoppe, N. S. Sariciftci, and D. Meissner, *Mol. Cryst. Liq. Cryst.* **385**, 113 (2002).
- ³⁰G. Xing, N. Mathews, S. S. Lim, N. Yantara, X. Liu, D. Sabba, M. Grätzel, S. Mhaisalkar, and T. C. Sum, *Nat. Mater.* **13**, 476 (2014).
- ³¹R. F. Pierret, *Advanced Semiconductor Fundamentals*, 2nd ed. (Prentice Hall, Upper Saddle River, New Jersey, 2002).
- ³²Taurus Medici (Software maker headquarters in 2010: Synopsys, 690 East Middlefield Road Mountain View, CA 94043 USA).
- ³³S. P. Bremner, M. Y. Levy, and C. B. Honsberg, *Prog. Photovoltaics Res. Appl.* **16**, 225 (2008).
- ³⁴A. Banerjee and S. Guha, *J. Appl. Phys.* **69**, 1030 (1991).
- ³⁵U. Feister and R. Grewe, *Photochem. Photobiol.* **62**, 736 (1995).